A G-equation formulation for large-eddy simulation of premixed turbulent combustion

By H. Pitsch

1. Motivation and objectives

Premixed turbulent combustion in technical devices often occurs in thin flame fronts. The propagation of these fronts, and hence, for instance, the heat release, are governed by the interaction of transport processes and chemistry within the front. In flamelet models this strong coupling is expressed by treating the flame front as a thin interface propagating with a laminar burning velocity s_L. The coupling of transport and chemistry is reflected in the scaling of the laminar burning velocity, which can be expressed as $s_L \sim \sqrt{D/t_c}$, where D is the diffusion coefficient and t_c is the chemical time scale. Flamelet models for premixed turbulent combustion have been extensively used in the past and different models have been formulated for Reynolds averaged (Bray *et al.* (1985); Peters (2000)) and large-eddy simulations (LES) (Hawkes & Cant (2000); Kim & Menon (2000); Chakravarthy & Menon (2001); Pitsch & Duchamp de Lageneste (2002)).

The G-equation model proposed by Williams (1985) is based on the flamelet modeling assumptions and uses a level-set method to describe the evolution of the flame front as an interface between the unburned and burned gases. The level-set function G is a scalar field defined such that the flame front position is at $G = G_0$, and that G is negative in the unburned mixture. The instantaneous and local G-equation can be derived by considering the instantaneous flame surface. An implicit representation of this surface can be given as

$$G(\boldsymbol{x}, t) - G_0 = 0\,, \tag{1.1}$$

which defines the level-set function G. Here, $\boldsymbol{x}$ is the vector of space coordinates. Differentiating Eq. (1.1), one obtains

$$\frac{\partial G}{\partial t} + \frac{d\boldsymbol{x}_f}{dt} \cdot \nabla G = 0\,, \tag{1.2}$$

where $\boldsymbol{x}_f$ is the flame front location. If the curvature radius of the instantaneous flame front is locally larger than the flame thickness, the flame is in the corrugated flamelets regime, and the flame front propagation speed is given by

$$\frac{d\boldsymbol{x}_f}{dt} = \boldsymbol{v} + s_L \boldsymbol{n}\,. \tag{1.3}$$

Here, $\boldsymbol{v}$ is the local flow velocity and s_L is the laminar burning velocity. The flame normal vector $\boldsymbol{n}$ is defined to be directed into the unburned mixture and can be expressed as

$$\boldsymbol{n} = -\frac{\nabla G}{|\nabla G|}\,. \tag{1.4}$$

Combining Eqs. (1.2) and (1.3) yields the instantaneous G-equation

$$\frac{\partial G}{\partial t} + \boldsymbol{v} \cdot \nabla G = s_L \, |\nabla G|\,. \tag{1.5}$$

Since this equation has been derived from Eqs. (1.1) and (1.3), which both only describe the flame surface, also Eq. (1.5) is valid at the flame surface only. The remaining G-field is arbitrary and commonly defined to be a distance function.

The location of G_0 can be defined to be anywhere in the flame, for instance at a given temperature iso-surface. Then, in Eq. (1.5), the velocity $\boldsymbol{v}$ is evaluated at that location, and the laminar burning velocity s_L has to be defined with respect to that location as well. Typically, G_0 is defined to be either immediately ahead of the flame in the unburned, or immediately behind the flame in the burned gases. The burning velocities defined with respect to the unburned and burned are denoted as $s_{L,u}$ and $s_{L,b}$, respectively.

Peters (1992, 1999, 2000) has developed an appropriate theory for premixed turbulent combustion describing the corrugated flamelets and the thin reaction zones regimes based on the G-equation formulation. Peters (2000) and Oberlack *et al.* (2001) pointed out that, since the G-field has physical meaning only at $G = G_0$, in order to derive the Reynolds averaged G-equation, conventional averaging of the G-field cannot be applied. For LES, this implies that not only is it impossible to obtain a filtered G-field from filtering the instantaneous resolved field, but also that the filter kernels, which are usually being used for filtering the velocity and scalar fields cannot be applied. In the application of the G-equation in LES, these facts have not been considered in the past. Hence, we first need to develop a filter kernel that takes information only from the instantaneous resolved flame surface. This will be done in the next section. Thereafter, the equation for the filtered flame front position will be derived. The resulting equation has two unclosed terms, a flame front conditionally averaged flow velocity appearing in the convection term, and the sub-filter burning velocity. To relate the conditional velocity to the unconditionally filtered velocity, which is known from the solution of the momentum equations, a model for this quantity will also be developed. Finally, we will derive an equation for the sub-filter flame front wrinkling, which will lead to an analytic model for the sub-filter burning velocity.

2. G-Equation for the filtered flame location valid in the corrugated flamelets regime

Peters (2000) and Oberlack *et al.* (2001) have pointed out that for the derivation of a G-equation for the ensemble or time averaged flame location the traditional averaging of the entire G-field cannot be applied. Because the G-field has physical significance only for $G = G_0$, only the G_0 iso-surface can be of relevance in the averaging procedure and the remaining G-field, which can be arbitrarily defined, must not be used. Instead, Peters (2000) has proposed an averaging procedure that only uses the probability density function (pdf) of finding $G = G_0$ at a particular location. This procedure was described only for the one-dimensional case. Oberlack *et al.* (2001) developed a rigorous averaging procedure for the three-dimensional case. Through the consistent application of this averaging procedure, a G-equation for the averaged flame location and an equation for the flame brush thickness have been derived for the corrugated flamelets regime. In this section, we will first develop an appropriate LES filter and then derive a G-equation for the filtered flame front location in the corrugated flamelets regime by using similar arguments as given by Oberlack *et al.* (2001). The resulting G-equation will be extended to the thin reaction zones regime in the following section.

A parametric representation of the flame surface $\mathcal{F}$ can be given as

$$\boldsymbol{x_f} = \boldsymbol{x_f}(\lambda, \mu, t)\,, \tag{2.1}$$

where $\boldsymbol{x}_f$ is the flame front location, and λ and μ are curvilinear coordinates along the flame surface forming an orthogonal coordinate system moving with the flame front. Considering a point P_0 on the flame surface, which is given by the coordinates (λ_0, μ_0), $\boldsymbol{x_f}(\lambda_0, \mu_0, t)$ describes the temporal development of the location of the point P_0 in physical space as function of time t. The coordinates λ and μ are hence parameters of the function $\boldsymbol{x}_f$ and will in the following be written as $\boldsymbol{\Lambda} = \binom{\lambda}{\mu}$.

For a given set of parameters $\boldsymbol{\Lambda}$, a spatial filter $\mathcal{H}$ can then be defined as

$$\mathcal{H}\left(\boldsymbol{\Lambda} - \boldsymbol{\Lambda}'\right) = \begin{cases} a(\boldsymbol{\Lambda}), & \text{if } \left|\boldsymbol{x}_f\left(\boldsymbol{\Lambda}\right) - \boldsymbol{x}_f\left(\boldsymbol{\Lambda}'\right)\right| \leq \frac{\boldsymbol{\Delta}}{2} \\ 0, & \text{otherwise} \end{cases}, \tag{2.2}$$

where $\boldsymbol{\Delta}$ is the filter width and $a(\boldsymbol{\Lambda})$ is a normalization factor that is determined by the normalization condition

$$\int_{\mathcal{F}} \mathcal{H}\left(\boldsymbol{\Lambda} - \boldsymbol{\Lambda}'\right) d\boldsymbol{\Lambda}' = 1\,. \tag{2.3}$$

This filter function is substantially different from the conventionally applied filter kernels for scalar quantities. Since the flame is only defined on a surface, the filter also has to move along this surface and cannot be used at an arbitrary point in space. The coordinates used in the filter function are therefore not spatial, but flame surface coordinates. Then, a spatial filtering operation for the flame front location can be defined as

$$\widehat{\boldsymbol{x}}_f\left(\boldsymbol{\Lambda}, t\right) = \int_{\mathcal{F}} \boldsymbol{x}_f\left(\boldsymbol{\Lambda'}, t\right) \mathcal{H}\left(\boldsymbol{\Lambda} - \boldsymbol{\Lambda}'\right) d\boldsymbol{\Lambda}'\,. \tag{2.4}$$

This filtering operation should be described in more detail for clarity. The surface coordinates $\boldsymbol{\Lambda}$ are defined along the instantaneous flame surface. To obtain the filtered front location, for each point $\boldsymbol{x}_f(\boldsymbol{\Lambda})$ on the instantaneous flame surface, the filtering operation Eq. (2.4) yields a corresponding mean flame front location $\widehat{\boldsymbol{x}}_f(\boldsymbol{\Lambda})$. These locations define the filtered flame front position. Note, that although $\widehat{\boldsymbol{x}}_f$ is expressed as a function of $\boldsymbol{\Lambda}$, these parameters are still defined through the unfiltered front.

Applying the filter operation to Eq. (1.3) leads to

$$\frac{d\widehat{\boldsymbol{x}}_f}{dt} = \widehat{\boldsymbol{v}} + \widehat{s_L \boldsymbol{n}}\,, \tag{2.5}$$

where the conditionally filtered flow velocity and propagation speed are given by

$$\widehat{\boldsymbol{v}}\left(\boldsymbol{\Lambda}, t\right) = \int_{\mathcal{F}} \boldsymbol{v}\left(\boldsymbol{\Lambda'}, t\right) \mathcal{H}\left(\boldsymbol{\Lambda} - \boldsymbol{\Lambda}'\right) d\boldsymbol{\Lambda}'\,. \tag{2.6}$$

and

$$\widehat{s_L \boldsymbol{n}}\left(\boldsymbol{\Lambda}, t\right) = \int_{\mathcal{F}} s_L\left(\boldsymbol{\Lambda'}, t\right) \boldsymbol{n}\left(\boldsymbol{\Lambda'}, t\right) \mathcal{H}\left(\boldsymbol{\Lambda} - \boldsymbol{\Lambda}'\right) d\boldsymbol{\Lambda}'\,. \tag{2.7}$$

To obtain an equation for the filtered flame front location, the implicit representation of the filtered flame surface, given as

$$\check{G}(\boldsymbol{x}, t) = G_0\,, \tag{2.8}$$

is differentiated and the displacement speed of $\check{G}$ appearing in this equation is associated

with the filtered displacement speed of the unfiltered front. This results in

$$\frac{\partial \check{G}}{\partial t} + \frac{d\widehat{\boldsymbol{x}}_f}{dt} \cdot \nabla \check{G} = 0\,. \tag{2.9}$$

Note that the $\widehat{\ }$-quantities are a direct result of the filtering operation Eq. (2.4), whereas $\check{G}$ is just the level-set representation of the filtered flame front location. Therefore, the filtered flame front is not yet defined by Eq. (2.8). Indeed, this equation and its differentiated form could describe any iso-surface. Only by choosing the propagation speed of this surface equal to the filtered propagation speed from Eq. (2.5), this surface is identified with the filtered flame front location. Introducing Eq. (2.5) into Eq. (2.9) yields the G-equation for the mean flame front location as

$$\frac{\partial \check{G}}{\partial t} + \widehat{\boldsymbol{v}} \cdot \nabla \check{G} = -\widehat{s_L \boldsymbol{n}} \cdot \nabla \check{G}\,. \tag{2.10}$$

As proposed by Oberlack *et al.* (2001), the propagation term defined in Eq. (2.7) can be modeled by the turbulent burning velocity, here the sub-grid burning velocity, s_T, and the gradient of the resolved G-field as

$$\widehat{s_L \boldsymbol{n}} = s_T \check{\boldsymbol{n}} = -s_T \frac{\nabla \check{G}}{\left|\nabla \check{G}\right|}\,, \tag{2.11}$$

where $\check{\boldsymbol{n}}$ is the normal vector of the filtered flame front position

$$\check{\boldsymbol{n}} = -\frac{\nabla \check{G}}{\left|\nabla \check{G}\right|}\,. \tag{2.12}$$

Note that according to the definition of G_0 the conditional velocity is either the filtered velocity in the immediate unburned or burned gases, which will be denoted by $\widehat{\boldsymbol{v}}_u$ and $\widehat{\boldsymbol{v}}_b$, respectively. Similarly, the turbulent burning velocity has to be defined with respect to the unburned or burned gases, denoted by $s_{T,u}$ and $s_{T,b}$. With these notations, depending on the definition of G_0, Eq. (2.10) can be written as either

$$\frac{\partial \check{G}}{\partial t} + \widehat{\boldsymbol{v}}_u \cdot \nabla \check{G} = s_{T,u} \left|\nabla \check{G}\right| \tag{2.13}$$

or

$$\frac{\partial \check{G}}{\partial t} + \widehat{\boldsymbol{v}}_b \cdot \nabla \check{G} = s_{T,b} \left|\nabla \check{G}\right|\,. \tag{2.14}$$

The evolution of the filtered flame front location can be described by either one of the Eqs. (2.13) and (2.14). To solve these equations, models for the sub-filter burning velocity and the flame front conditioned, filtered velocity have to be provided. The latter quantity has to be modeled in terms of the Favre-filtered velocities, which are known from the solution of the Favre-filtered momentum equations. Models for these quantities will be provided in subsequent sections.

3. *G*-equation for the filtered flame location valid in the corrugated flamelets and the thin reaction zones regime

In the derivation for the instantaneous G-equation for the thin reaction zones regime, Peters (2000) starts from the instantaneous temperature equation and develops a level-set equation for a temperature iso-surface given by $T(\boldsymbol{x}, t) = T^0$, where T^0 is the inner layer

temperature. The expression for the propagation speed is similar to Eq. (1.3), where, following Gibson (1968), the displacement speed, s_d, can be written as

$$s_d = \left(\frac{\nabla \cdot (\rho D_T \nabla T) + \omega_T}{\rho |\nabla T|} \right)_{T=T^0} . \tag{3.1}$$

Here, ρ is the density, D_T is the temperature diffusivity, and ω_T is the chemical source term. With the temperature iso-surface normal vector $\boldsymbol{n}_T = -\nabla T/|\nabla T|$, the transport term in Eq. (3.1) can be expressed by its components normal and tangential to the T^0 surface and the displacement speed becomes

$$s_d = -\left(D_T \nabla \cdot \boldsymbol{n}_T\right)_{T=T^0} + \left(\frac{-\boldsymbol{n}_T \left(\rho D_T |\nabla T|\right) - \omega_T}{|\nabla T|} \right)_{T=T^0} = s_\kappa + (s_n + s_r) . \tag{3.2}$$

Peters *et al.* (1998) have shown that $(s_n + s_r)$, which for an unstrained premixed flame is the laminar burning velocity, is not significantly changed by turbulence, and therefore, in the thin reaction zones regime, is small compared with the contribution from curvature s_κ. Since the temperature iso-surface $T = T^0$ will be described by $G = G_0$, s_κ can be written as

$$s_\kappa = -D_T \nabla \cdot \boldsymbol{n} = D_T \nabla \cdot \left(\frac{\nabla G}{|\nabla G|} \right) . \tag{3.3}$$

The combined displacement velocity valid in the corrugated flamelets and the thin reaction zones regime is given by an expression similar to Eq. (1.3), but with the laminar burning velocity s_L replaced by $s_L + s_\kappa$. Filtering this expression with the filter operation given by Eq. (2.4) leads to

$$\frac{d\widehat{\boldsymbol{x}}_f}{dt} = \widehat{\boldsymbol{v}} + \widehat{(s_L + s_\kappa)\,\boldsymbol{n}} . \tag{3.4}$$

Introducing Eq. (3.4) into Eq. (2.9) leads to the G-equation valid for the corrugated flamelets and the thin reaction zones regime

$$\frac{\partial \check{G}}{\partial t} + \widehat{\boldsymbol{v}} \cdot \nabla \check{G} = -\widehat{(s_L + s_\kappa)\,\boldsymbol{n}} \cdot \nabla \check{G} . \tag{3.5}$$

As in Eq. (2.11), the propagation term can again be modeled by a turbulent burning velocity and the normal vector of the mean flame front position as

$$\widehat{(s_L + s_\kappa)\,\boldsymbol{n}} = s_T \check{\boldsymbol{n}} = -s_T \frac{\nabla \check{G}}{|\nabla \check{G}|} . \tag{3.6}$$

It is important to note that in the modeling of the turbulent burning velocity, the effect of curvature, most important in the small scale turbulence regime, and the effect of laminar flame propagation, important in the large scale turbulence regime, have to be considered. It is also interesting to note that in the present derivation of the G-equation, the term proportional to the eddy diffusivity and the curvature of the mean field, which in Peters (2000) and Pitsch & Duchamp de Lageneste (2002) arises from the scalar flux term in the thin reaction zones regime, does not appear. This term always leads to a stabilization of the mean flame front and hence, to a decrease in the resolved scale turbulent burning velocity.

4. Model for the conditionally filtered flow velocity

A consistency requirement for the conditional velocities model is imposed by the fact that Eqs. (2.13) and (2.14) are equivalent. After applying a model for $\widehat{\boldsymbol{v}}_u$ in Eq. (2.13) and $\widehat{\boldsymbol{v}}_b$ in Eq. (2.14), these still have to have the same solution. In the following, we will therefore first develop a model for the conditional velocities, and then show that applying the model to both equations leads to equivalent formulations.

The conditional velocity $\widehat{\boldsymbol{v}}$ is the velocity at the flame front, weighted with the filter function $\mathcal{H}$ and averaged over the entire flame surface within the filter volume. Physically, this averaged velocity, as it appears in the convection term in Eq. (2.10), leads to the convection of the entire sub-filter flame surface. Hence, it is important only to capture the large-scale velocity motion in the model for the conditional velocities, and not the small scale velocity fluctuations, which only lead to sub-grid flame wrinkling, but not to convection on the resolved scales. Then, the local unfiltered velocities can be assumed to be constant in the burned and the unburned part of the sub-filter volume. These velocities are then equal to the respective conditional velocities. This can be written as

$$\boldsymbol{v}(G) = \begin{cases} \widehat{\boldsymbol{v}}_u & \text{if } G < G_0 \\ \widehat{\boldsymbol{v}}_u & \text{if } G = G_0 \text{ and } G_0 \text{ defined in the unburned} \\ \widehat{\boldsymbol{v}}_b & \text{if } G = G_0 \text{ and } G_0 \text{ defined in the burned} \\ \widehat{\boldsymbol{v}}_b, & \text{if } G > G_0 \end{cases} , \tag{4.1}$$

where it has to be distinguished, whether G_0 is defined to be in the unburned or the burned mixture. The unconditional Favre-filtered velocity can then be expressed by

$$\overline{\rho}\widetilde{\boldsymbol{v}} = \int_{-\infty}^{\infty} \rho \boldsymbol{v}(G) P(G) dG = \rho_u \widehat{\boldsymbol{v}}_u \int_{-\infty}^{G_0} P(G) dG + \rho_b \widehat{\boldsymbol{v}}_b \int_{G_0}^{\infty} P(G) dG \,, \tag{4.2}$$

where $P(G)$ is the pdf of finding a particular value of G. Introducing the probability of finding burned mixture as

$$p_b = \int_{G_0}^{\infty} P(G) dG \,, \tag{4.3}$$

the unconditional velocity can be written as

$$\overline{\rho}\widetilde{\boldsymbol{v}} = \rho_u \widehat{\boldsymbol{v}}_u (1 - p_b) + \rho_b \widehat{\boldsymbol{v}}_b p_b \,. \tag{4.4}$$

Similarly, the unconditionally filtered density can be derived as

$$\overline{\rho} = \rho_u (1 - p_b) + \rho_b p_b \,. \tag{4.5}$$

To express $\widehat{\boldsymbol{v}}_b$ by $\widehat{\boldsymbol{v}}_u$, we will use the jump condition for the mass balance across the mean flame interface, given by

$$\rho_u \check{\boldsymbol{n}} \cdot \left(\widehat{\boldsymbol{v}}_u - \frac{\partial \widehat{\boldsymbol{x}}_f}{\partial t} \right) = \rho_b \check{\boldsymbol{n}} \cdot \left(\widehat{\boldsymbol{v}}_b - \frac{\partial \widehat{\boldsymbol{x}}_f}{\partial t} \right) . \tag{4.6}$$

The displacement speed can be expressed by Eqs. (3.4) and (3.6), where the choice of the conditional velocity and the burning velocity depend on the location of G_0 with respect to the flame. If G_0 is defined to be in the unburned mixture, $\widehat{\boldsymbol{v}}_u$ and $s_{T,u}$ have to be used. However, if G_0 is in the burned gases, then the appropriate values are given by $\widehat{\boldsymbol{v}}_b$

and $s_{T,b}$. For the velocity jump across the flame front this results in

$$\check{\boldsymbol{n}} \cdot (\widehat{\boldsymbol{v}}_u - \widehat{\boldsymbol{v}}_b) = \frac{\rho_u - \rho_b}{\rho_b} s_{T,u} \,, \tag{4.7}$$

if G_0 is defined to be in the unburned mixture, and

$$\check{\boldsymbol{n}} \cdot (\widehat{\boldsymbol{v}}_u - \widehat{\boldsymbol{v}}_b) = \frac{\rho_u - \rho_b}{\rho_u} s_{T,b} \,, \tag{4.8}$$

if G_0 is in the burned gases. Introducing Eqs. (4.7) and (4.8) into Eq. (4.4) results in expressions for the conditional velocities in terms of the unconditional velocities as

$$\check{\boldsymbol{n}} \cdot \widehat{\boldsymbol{v}}_u = \check{\boldsymbol{n}} \cdot \widetilde{\boldsymbol{v}} + \frac{\rho_u - \rho_b}{\overline{\rho}} s_{T,u} p_b \tag{4.9}$$

and

$$\check{\boldsymbol{n}} \cdot \widehat{\boldsymbol{v}}_b = \check{\boldsymbol{n}} \cdot \widetilde{\boldsymbol{v}} - \frac{\rho_u - \rho_b}{\overline{\rho}} s_{T,b} \left(1 - p_b\right) \,. \tag{4.10}$$

In order to make use of these relations in the G-equation given by Eqs. (2.13) and (2.14), we first split the convection term into a flame normal and a flame tangential part. Since the flame tangential part only leads to a parallel translation of the flame front and has no influence on the flame propagation, it can be neglected. The convection term from Eq. (2.13), for instance, can then be written as

$$\widehat{\boldsymbol{v}}_u \cdot \nabla \check{G} = \left(\check{\boldsymbol{n}} \cdot \widehat{\boldsymbol{v}}_u\right) \check{\boldsymbol{n}} \cdot \nabla \check{G} \,. \tag{4.11}$$

After introducing Eq. (4.9) into the normal convection term, only the normal component of the unconditional velocity appears, which can again be complemented by the tangential part without changing the solution, which leads to

$$\frac{\partial \check{G}}{\partial t} + \widetilde{\boldsymbol{v}} \cdot \nabla \check{G} = s_{T,u} \left|\nabla \check{G}\right| \left(1 + \frac{\rho_u - \rho_b}{\overline{\rho}} p_b\right) \tag{4.12}$$

and

$$\frac{\partial \check{G}}{\partial t} + \widetilde{\boldsymbol{v}} \cdot \nabla \check{G} = s_{T,b} \left|\nabla \check{G}\right| \left(1 - \frac{\rho_u - \rho_b}{\overline{\rho}} \left(1 - p_b\right)\right) \,. \tag{4.13}$$

With Eq. (4.5), the equations for the filtered flame front position can be written as

$$\frac{\partial \check{G}}{\partial t} + \widetilde{\boldsymbol{v}} \cdot \nabla \check{G} = \frac{\rho_u}{\overline{\rho}} s_{T,u} \left|\nabla \check{G}\right| \tag{4.14}$$

and

$$\frac{\partial \check{G}}{\partial t} + \widetilde{\boldsymbol{v}} \cdot \nabla \check{G} = \frac{\rho_b}{\overline{\rho}} s_{T,b} \left|\nabla \check{G}\right| \,. \tag{4.15}$$

It is easily seen that these equations satisfy some important limits. If Eq. (4.14) is evaluated in the unburned mixture, then $\widetilde{\boldsymbol{v}} = \widehat{\boldsymbol{v}}_u$ and $\overline{\rho} = \rho_u$. Hence, Eq. (2.13) is recovered. If, on the other hand, this equation is evaluated in the burned gases, $\widetilde{\boldsymbol{v}} = \widehat{\boldsymbol{v}}_b$, $\overline{\rho} = \rho_b$, and, since the mass conservation through the flame requires

$$\rho_u s_{T,u} = \rho_b s_{T,b} \,, \tag{4.16}$$

the right hand side goes to $s_{T,b} \left|\nabla \check{G}\right|$. Therefore, in the burned gases, Eq. (2.14) is recovered. By using Eq. (4.16), it can also be shown easily that Eqs. (4.14) and (4.15) are equivalent.

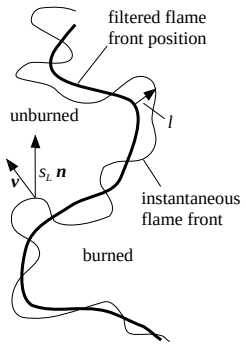

FIGURE 1. Instantaneous and filtered flame front position

5. Equation for the sub-filter flame brush thickness

We now want to derive an equation for the length-scale of the sub-filter flame front fluctuations l, which might be associated with the sub-filter flame brush thickness. This equation will then be used to derive a model for the turbulent burning velocity. The flame front fluctuation l will here be defined as the distance of the instantaneous flame front to the filtered flame front in the direction normal to the filtered flame surface, as indicated in Fig. 1. Then, l is simply the distance between the points $\boldsymbol{x}_f$ and $\widehat{\boldsymbol{x}}_f$ given by

$$l = |\boldsymbol{x}_f - \widehat{\boldsymbol{x}}_f| \; . \tag{5.1}$$

For a given point $\widehat{\boldsymbol{x}}_f$ on the filtered flame surface, the appropriate location on the instantaneous surface is then defined with the filtered front normal vector at $\widehat{\boldsymbol{x}}_f$ as

$$l\,\check{\boldsymbol{n}} = \boldsymbol{x}_f - \widehat{\boldsymbol{x}}_f \; . \tag{5.2}$$

It is easy to see that this definition of the length scale satisfies the important criterion that l tends to zero, if the flame front wrinkling is completely resolved, since this implies that $\boldsymbol{x}_f$ and $\widehat{\boldsymbol{x}}_f$ are the same. Other choices could be made to define the length-scale of the sub-filter flame front wrinkling. For instance, the length-scale could be evaluated at constant value of Λ as $\boldsymbol{l} = \boldsymbol{x}_f(\Lambda) - \widehat{\boldsymbol{x}}_f(\Lambda)$, which would correspond to the definition used in Oberlack *et al.* (2001). However, this definition does not necessarily tend to zero, if the flame is resolved.

Similar to the G-variance equation given in Peters (2000), the equation for flame front fluctuations has a production term, active on the large scales, and two dissipation terms, the kinematic restoration term, important in the corrugated flamelets regime, and the scalar dissipation term, important in the thin reaction zones regime. The length scale equation should therefore actually be derived and modeled separately in each of these regimes and combined subsequently. Here, for brevity, only the combined equation, valid in both regimes, will be derived. However, the modeling of each dissipation term will be done in the limit, where only this particular term is important.

Differentiating Eq. (5.2) and using Eq. (3.4) and the corresponding unfiltered equation, an expression for l can be derived as

$$\frac{dl\,\check{\boldsymbol{n}}}{dt} = \frac{d\boldsymbol{x}_f - \widehat{\boldsymbol{x}}_f}{dt} = \boldsymbol{v} - \widehat{\boldsymbol{v}} + s_L\boldsymbol{n} - \widehat{s_L\boldsymbol{n}} + s_\kappa\boldsymbol{n} - \widehat{s_\kappa\boldsymbol{n}} \, . \tag{5.3}$$

The equation for the length scale of the sub-filter flame front fluctuations can then be obtained by multiplying Eq. (5.3) by $l\,\check{\boldsymbol{n}}$ and applying the filtering operation, given by

Eq. (2.4). This leads to

$$\frac{d\widehat{l^2}}{dt} = 2\widehat{\check{\boldsymbol{n}} \cdot l\boldsymbol{v'}} + 2\widehat{\check{\boldsymbol{n}} \cdot l(s_L\boldsymbol{n})'} + 2\widehat{\check{\boldsymbol{n}} \cdot l(s_\kappa\boldsymbol{n})'}\,, \tag{5.4}$$

where the sub-filter velocity fluctuation has been introduced as $\boldsymbol{v'} = \boldsymbol{v} - \widehat{\boldsymbol{v}}$ and the turbulent burning velocity fluctuations as $(s_L\boldsymbol{n})' = s_L\boldsymbol{n} - \widehat{s_L\boldsymbol{n}}$ and $(s_\kappa\boldsymbol{n})' = s_\kappa\boldsymbol{n} - \widehat{s_\kappa\boldsymbol{n}}$. Since $\widehat{l^2}$ is a quantity that is defined at the filtered flame front only, the rate of change can be described in an Eulerian frame of reference such that

$$\frac{d\widehat{l^2}}{dt} = \frac{\partial\widehat{l^2}}{\partial t} + \frac{d\widehat{\boldsymbol{x}}_f}{dt} \cdot \nabla\widehat{l^2}\,, \tag{5.5}$$

which, using Eq. (2.5), leads to

$$\frac{\partial\widehat{l^2}}{\partial t} + (\widehat{\boldsymbol{v}} + \widehat{s_L\boldsymbol{n}}) \cdot \nabla\widehat{l^2} = 2\widehat{\check{\boldsymbol{n}} \cdot l\boldsymbol{v'}} + 2\widehat{\check{\boldsymbol{n}} \cdot l(s_L\boldsymbol{n})'} + 2\widehat{\check{\boldsymbol{n}} \cdot l(s_\kappa\boldsymbol{n})'}\,. \tag{5.6}$$

The convective transport term can again be modeled as described earlier using Eqs. (2.11) and (4.9), which leads to

$$\frac{\partial\widehat{l^2}}{\partial t} + \left(\widetilde{\boldsymbol{v}} + \frac{\rho_u}{\overline{\rho}} s_T\check{\boldsymbol{n}}\right) \cdot \nabla\widehat{l^2} = 2\widehat{\check{\boldsymbol{n}} \cdot l\boldsymbol{v'}} + 2\widehat{\check{\boldsymbol{n}} \cdot l(s_L\boldsymbol{n})'} + 2\widehat{\check{\boldsymbol{n}} \cdot l(s_\kappa\boldsymbol{n})'}\,. \tag{5.7}$$

In Eq. (5.7), the terms on the left hand side describe the rate of change and the transport of the length scale due to the flame displacement. The first term on the right hand side describes the production of flame front wrinkling due to the turbulence, whereas the second and third terms on the right hand side are the flame surface dissipation due to flame propagation and diffusive curvature effects, respectively.

To model the production term in Eq. (5.7), we have to consider the scalar flux term $\widehat{\check{\boldsymbol{n}} \cdot l\boldsymbol{v'}}$, which would typically be expressed using a gradient transport assumption, involving a turbulent eddy viscosity and the spatial gradient of the scalar. However, since the flame front fluctuation l is defined at the mean flame front position only, spatial gradients of this quantity are not defined. The length scale l will therefore first be related to fluctuations of the scalar field G, which for small l or constant $|\nabla\check{G}|$ around the flame front can be written as

$$l = \frac{G'}{|\nabla\check{G}|}\,. \tag{5.8}$$

Note that constant $|\nabla\check{G}|$ can be required, because the definition of the $\check{G}$-field away from $\check{G} = G_0$ is arbitrary, and that l is certainly still independent of the definition of this field. The scalar flux term then becomes

$$\widehat{\check{\boldsymbol{n}} \cdot l\boldsymbol{v'}} = \widehat{\frac{\check{\boldsymbol{n}}}{|\nabla\check{G}|} \cdot G'\boldsymbol{v'}} = -\frac{\check{\boldsymbol{n}}}{|\nabla\check{G}|} D_{t,G} \cdot \nabla\check{G}\,, \tag{5.9}$$

where the right hand side has been obtained by invoking a gradient transport assumption for G. With the definition of the mean flame front normal vector, Eq. (2.12), the turbulent production term can then be modeled by

$$\widehat{\check{\boldsymbol{n}} \cdot l\boldsymbol{v'}} = D_{t,G}\,. \tag{5.10}$$

$D_{t,G}$ would generally be called the eddy diffusivity of G. This is misleading, since the scalar G is non-diffusive. However, $D_{t,G}$ appears not in a diffusion type term in the

modeled form of the length scale equation, but as a source term, which, since a turbulent diffusivity really describes turbulent transport rather than diffusion, accounts for the production of flame surface through turbulent mixing. This also implies that $D_{t,G}$ has no contribution from a molecular diffusion coefficient. It should therefore be called turbulent transport coefficient rather than eddy diffusivity. Since the definition of G outside $G = G_0$ is arbitrary, this coefficient cannot be simply determined using the dynamic procedure for scalar quantities as proposed by Moin *et al.* (1991). Instead, a constant Schmidt number assumption with a Smagorinsky-type model for the sub-filter eddy viscosity will be used for $D_{t,G}$, which results in

$$D_{t,G} = \frac{C_\nu \Delta v'_\Delta}{\mathrm{Sc}_{t,G}}\,, \tag{5.11}$$

where $C_\nu\Delta$ is a sub-filter length-scale given by the filter width Δ and the Smagorinsky coefficient C_ν, the latter of which is determined by a dynamic model as described by Moin *et al.* (1991). According to Pitsch & Steiner (2000), the Schmidt number has been chosen to be $\mathrm{Sc}_{t,G} = 0.5$.

Since both dissipation terms act on the small scales, the scaling relations for these terms provided by Peters (1999) in a Reynolds averaged context can also be applied here. In the corrugated flamelets regime, the kinematic restoration term is the dominant dissipation term. This term should be independent of small scale quantities such as the laminar burning velocity, but scales with the mean propagation term and can be expressed as

$$\widehat{\check{\boldsymbol{n}} \cdot l(s_L \boldsymbol{n})'} = c_2 C_\nu \Delta\, \check{\boldsymbol{n}} \cdot \widehat{s_L \boldsymbol{n}} = -c_2 C_\nu \Delta\, s_T\,, \tag{5.12}$$

where the turbulent burning velocity has been introduced using Eq. (2.11).

Similarly, also the scalar dissipation term, dominant in the thin reaction zones regime, is assumed to scale with the respective mean propagation term. Since a dissipation term can be written independently of the large scales, the missing length scale is obtained from the small scale quantities and it follows

$$\widehat{\check{\boldsymbol{n}} \cdot l(s_\kappa \boldsymbol{n})'} = c_1 \frac{l_F}{s_L} \left(\check{\boldsymbol{n}} \cdot \widehat{s_\kappa \boldsymbol{n}}\right)^2 = -c_3 \frac{l_F}{s_L} s_T^2\,. \tag{5.13}$$

Introducing Eqs. (5.10), (5.12), and (5.13) into Eq. (5.7), and assuming that production equals dissipation in that equation, an expression for the turbulent burning velocity can be obtained as

$$D_{t,G} - c_2 C_\nu \Delta\, s_T - c_3 \frac{l_F}{s_L} s_T^2 = 0\,. \tag{5.14}$$

This leads to

$$\frac{s_T - s_L}{s_L} = -\frac{b_3^2 C_\nu}{2 b_1 \mathrm{Sc}_{t,G}} \frac{\Delta}{l_F} + \sqrt{\left(\frac{b_3^2 C_\nu}{2 b_1 \mathrm{Sc}_{t,G}} \frac{\Delta}{l_F}\right)^2 + \frac{b_3^2 D_t}{s_L l_F}}\,. \tag{5.15}$$

Here, the laminar burning velocity has been added to satisfy the laminar limit. The constants c_2 and c_3 have been determined such that Eq. (5.15) results for $\Delta/l_F \to 0$ in Damköhler's small-scale limit

$$\frac{s_T - s_L}{s_L} = b_1 \frac{v'_\Delta}{s_L}\,, \tag{5.16}$$

and for $\Delta/l_F \to \infty$ in the large-scale limit

$$\frac{s_T - s_L}{s_L} = b_3 \sqrt{\frac{D_t}{D}}\,. \tag{5.17}$$

The resulting expressions for the constants are $c_2 = 1/(b_1 \mathrm{Sc}_{t,G})$ and $c_3 = 1/b_3^2$, where the constants b_1 and b_3 have been taken from Peters (2000) to be $b_1 = 2.0$ and $b_3 = 1.0$.

Finally, in light of these results, the scaling used in the modeling of the dissipation terms in the length scale equation should be discussed. To derive the models given in Eqs. (5.12) and (5.13), dimensional arguments have been used, which, if used differently, could also have led to different results. In particular, for the kinematic restoration, a linear dependence of the propagation term has been assumed, while for the scalar dissipation term a quadratic dependence is used. As an example for a different scaling possibility, the latter could also have been expressed as linearly dependent on the propagation term times the small scale length scale l_F. Such a scaling has been used in Pitsch & Duchamp de Lageneste (2002), which then led to a similar, but different expression for the turbulent burning velocity. The quadratic relation, which for the scaling used in this study is given by Eq. (5.14), has then no linear term, and can be solved more easily. However, the choice of the particular scaling used here and also in Peters (2000) is motivated by results from direct numerical simulations by Wenzel (2000), who studied the evolution of the G-equation in forced isotropic turbulence. Unfortunately, the scaling of the dissipation terms in the length scale equation has not been investigated, but the scaling of the corresponding terms in an equation for the flame surface area ratio $\sigma = |\nabla G|$ has been given. It is found that the kinematic restoration term depends quadratically, the scalar dissipation rate cubicly on σ. These dependencies can be translated to the length scale equation. Since $\sigma \sim G'$, it follows that $\frac{dG'^2}{G'^2} \sim \frac{d\sigma}{\sigma}$, which, using Eq. (5.8), leads to $dl^2 = \frac{G'^2}{\sigma} d\sigma$. This shows that compared with the transport equation for σ given in Peters (2000), in the equation for l^2, given by Eq. (5.7), the power of σ in the dissipation terms should be decreased by one. This results in the scaling employed in Eqs. (5.12) and (5.13), since, using the present filtering procedure, σ appears in form of the normal vector.

6. Conclusions and future work

In the present paper a consistent formulation of the G-equation approach for LES has been developed. It has been discussed that the instantaneous unfiltered G-equation is valid only at the instantaneous flame front location. In a filtering procedure, applied to derive the appropriate LES equation, only states on the instantaneous unfiltered flame surface can hence be considered. A new filter kernel has been provided here that averages only states along the flame surface. The filter has been used to derive the G-equation for the filtered flame front location. This equation has two unclosed terms involving a flame front conditionally averaged flow velocity and a turbulent burning velocity. A model for the conditional velocity is derived expressing this quantity in terms of the Favre-filtered flow velocity, which is usually known from the flow solver. This model leads to the appearance of a density ratio in the propagation term of the G-equation. Due to the application of the new filtering procedure, also a propagation term proportional to the curvature of the mean front does not appear. This is an important difference to the mean G-equation given by Pitsch & Duchamp de Lageneste (2002), since the term has a stabilizing effect on the flame front and will therefore lead to a decreased resolved

turbulent burning velocity. An equation for the length-scale of the sub-filter flame front wrinkling is derived and leads to a model for the turbulent burning velocity. In the future, we will validate the present formulation in LES of turbulent premixed combustion experiments and assess the importance of the differences in the present formulation. Also, having provided a sound filtering procedure, dynamic models for the turbulent burning velocity can now be developed.

7. Acknowledgments

The authors gratefully acknowledge funding by the US Department of Energy within the ASCI program and by Snecma Moteurs. The author also thanks Marcus Herrmann for many inspiring discussions.

REFERENCES

Bray, K. N. C., Libby, P. A. & Moss, J. B. 1985 Unified modeling approach for premixed turbulent combustion. 1. general formulation. *Combust. Flame* **61**, 87–102.

Chakravarthy, V. K. & Menon, S. 2001 Large-eddy simulation of turbulent premixed flames in the flamelet regime. *Comb. Sci. Tech.* **162**, 175.

Gibson, C. H. 1968 Fine structure of scalar fields mixed ty turbulence. I. Zero-gradient points and minimal gradient surfaces. *Phys. Fluids* **11**, 2305.

Hawkes, E. R. & Cant, R. S. 2000 A flame surface density approach to large-eddy simulation of premixed turbulent combustion. *Proc. Combust. Inst.* **28**, 51–58.

Kim, W. W. & Menon, S. 2000 Numerical modeling of turbulent premixed flames in the thin-reaction-zones regime. *Comb. Sci. Tech.* **160**, 119–150.

Moin, P., Squires, K., Cabot, W. & Lee, S. 1991 A dynamic subgrid-scale model for compressible turbulence and scalar transport. *Phys. Fluids A* **3**, 2746–2757.

Oberlack, M., Wenzel, H. & Peters, N. 2001 On symmetries and averaging of the G-equation for premixed combustion. *Comb. Theory Modelling* **5** (4), 1–20.

Peters, N. 1992 A spectral closure for premixed turbulent combustion in the flamelet regime. *J. Fluid Mech.* **242**, 611–629.

Peters, N. 1999 The turbulent burning velocity for large scale and small scale turbulence. *J. Fluid Mech.* **384**, 107–132.

Peters, N. 2000 *Turbulent Combustion*. Cambridge University Press.

Peters, N., Terhoeven, P., Chen, J. H. & Echekki, T. 1998 Statistics of flame displacement speeds from computations of $2-d$ unsteady methane-air flames. *Proc. Combust. Inst.* **27**, 833–839.

Pitsch, H. & Duchamp de Lageneste, L. 2002 Large-eddy simulation of premixed turbulent combustion using a level-set approach. *Proc. Combust. Inst.* **29**, accepted for publication.

Pitsch, H. & Steiner, H. 2000 Large-eddy simulation of a turbulent piloted methane/air diffusion flame (Sandia flame D). *Phys. Fluids* **12** (10), 2541–2554.

Wenzel, H. 2000 Direkte numerische Simulation der Ausbreitung einer Flammenfront in einem homogenen Turbulenzfeld. PhD thesis, RWTH Aachen.

Williams, F. A. 1985 Turbulent combustion. In *The Mathematics of Combustion* (ed. J. D. Buckmaster), pp. 197–1318. Society for Industrial & Applied Mathematics.